Technical University of Denmark

DTU

Airfoil Computations using the - Re Model

Sørensen, Niels N.

Publication date:
2009

Document Version
Publisher's PDF, also known as Version of record

Link back to DTU Orbit

Citation (APA):
Sørensen, N. N. (2009). Airfoil Computations using the - Re Model. Roskilde: Danmarks Tekniske Universitet, Risø Nationallaboratoriet for Bæredygtig Energi. (Denmark. Forskningscenter Risoe. Risoe-R; No. 1693(EN)).

DTU Library
Technical Information Center of Denmark

Airfoil Computations using the γ - Re_θ Model

Risø-R-Report

Niels N. Sørensen
Risø-R-1693(EN)
July 2009

Author: Niels N. Sørensen

Title: Airfoil Computations using the $\gamma - Re_\theta$ Model

Department: Aeroelastic Design – Wind Energy Department

Abstract:

The present work addresses the validation of the implementation of the Menter, Langtry et al. $\gamma - \theta$ corrrelation based transition model [1, 2, 3] in the EllipSys2D code. Firstly the 2. order of accuracy of the code is verified using a grid refinement study for laminar, turbulent and transitional computations. Based on this, an estimate of the error in the computations is determined to be approximately one percent in the attached region. Following the verification of the implemented model, the model is applied to four airfoils, NACA64-018, NACA64-218, NACA64-418 and NACA64-618 and the results are compared to measurements [4] and computations using the Xfoil code by Drela et al. [5]. In the linear pre stall region good agreement is observed both for lift and drag, while differences to both measurements and Xfoil computations are observed in stalled conditions.

Contents

1   Introduction

The present work addresses the validation of the implementation of the Menter, Langtry et al. $\gamma - \theta$ corrrelation based transition model [1, 2, 3] in the EllipSys2D code. Firstly the 2. order of accuracy of the code is verified using a grid refinement study for laminar, turbulent and transitional computations. Based on this, an estimate of the error in the computations is determined to be approximately one percent in the attached region. Following the verification of the implemented model, the model is applied to four airfoils, NACA64-018, NACA64-218, NACA64-418 and NACA64-618 and the results are compared to measurements [4] and computations using the Xfoil code by Drela et al. [5]. In the linear pre stall region good agreement is observed both for lift and drag, while differences to both measurements and Xfoil computations are observed in stalled conditions.

2   Flow solver

The in-house flow solver EllipSys2D is used in all computations presented in the present work. The code is developed in co-operation between the Department of Mechanical Engineering at the Technical University of Denmark and The Department of Wind Energy at Risø National Laboratory, see [6, 7] and [8]. The EllipSys3D code is a multiblock finite volume discretization of the incompressible Reynolds Averaged Navier-Stokes (RANS) equations in general curvilinear coordinates. The code uses a collocated variable arrangement, and Rhie/Chow interpolation [9] is used to avoid odd/even pressure decoupling. As the code solves the incompressible flow equations, no equation of state exists for the pressure, and in the present work the SIMPLE algorithm of Patankar and Spalding [10, 11] or the PISO algorithm of Issa [12, 13] is used to enforce the pressure/velocity coupling, for steady state and transient computations, respectively. The EllipSys3D code is parallelized with MPI for executions on distributed memory machines, using a non-overlapping domain decomposition technique.

Both steady state and unsteady computations can be performed. For the unsteady computations the solution is advanced in time using a 2nd order iterative time-stepping (or dual time-stepping) method. In each global time-step the equations are solved in an iterative manner, using under relaxation. First, the momentum equations are used as a predictor to advance the solution in time. At this point in the computation the flowfield will not fulfil the continuity equation. The rewritten continuity equation (the so-called pressure correction equation) is used as a corrector making the predicted flowfield satisfy the continuity constraint. This two step procedure corresponds to a single sub-iteration, and the process is repeated until a convergent solution is obtained for the time step. When a convergent solution is obtained, the variables are updated, and we continue with the next time step. Thus, when the sub-iteration process is finished all terms are evaluated at the new time level.

For steady state computations, which is used in the present work, the global time-step is set to infinity and dual time stepping is not used, this corresponds to the use of local time stepping. In order to accelerate the overall algorithm, a multi-level grid sequence is used in the steady state computations. The convective terms are discretized using a third order QUICK upwind scheme, implemented using the deferred correction approach first suggested by Khosla and Rubin [14]. Central differences are used for the viscous terms, in each sub-iteration only the normal terms are treated fully implicit, while the terms from non-orthogonality and the variable viscosity terms are treated explicitly.

In the present work the turbulence in the boundary layer is modeled by the k-ω SST eddy viscosity model [15]. The equations for the turbulence model and the transition model are solved after the momentum and pressure correction equations in every sub-iteration/pseudo

time step, and in agreement with the recommendations of Menter et al. [1], a second order upwind TVD scheme based on the MinMod limiter is used for the transport equations for turbulence and transition. The three momentum equations, the $k - \omega$ equations and the two transition model equations are solved decoupled using a red/black Gauss-Seidel point solver. The solution of the Poisson system arising from the pressure correction equation is accelerated using a multigrid method.

3 Accuracy

The standard way of estimating the accuracy of a code is using Richardson Extrapolation on successive refinements of the grid, doubling the number of points in all directions. The actual order of the code (p) for the given problem can be estimated using

$$p = \log\left(\frac{U3 - U2}{U2 - U1}\right)\frac{1}{\log(r)} \ , \ r = 2 \ . \tag{1}$$

In the above formula, the refinement ratio (r) is the grid spacing on the coarser level divided with the grid spacing of the next finer level. $U3$, $U2$ and $U1$ are the solutions on the coarse, medium and finest coarsening of the grid, respectively. The present formula, assumes that the error is dominated by a term with constant order over the total range of grid refinements. Using the third order QUICK scheme for the convective terms, and the second order accurate central differencing scheme for the diffusive terms, we deal with a so-called mixed-order numerical scheme, (being defined as a scheme "where two terms different order in the truncation error are of similar magnitude over the range of mesh densities examined", see [16]. Assuming, that the scheme is a mix of a second and a third order scheme we get:

$$f_{exact} = f_{comp} + g_1 h^2 + g_2 h^3 + O(h^4) \ . \tag{2}$$

Having the solution on three grid levels, the exact solution (f_{exact}), and the coefficient for the second and third order terms (g_1 and g_2) can be estimated from the following expressions:

$$f_{exact} = \frac{32 f_{c1} - 12 f_{c2} + f_{c3}}{21} \ , \tag{3}$$

$$g_1 = \frac{7 f_{exact} - 8 f_{c1} + f_{c2}}{4h^2} \ , \tag{4}$$

$$g_2 = \frac{4 f_{c1} - f_{c2} - 3 f_{exact}}{4h^3} \ . \tag{5}$$

Where f_{c1}, f_{c2} and f_{c3} are the solutions on the fine, coarse and medium levels, respectively. Using the mixed-order analysis, it is possible to judge the size the second and third order terms.

Using a fine grid of 1024×384 cells, with a wall spacing of 1×10^{-7} chord lengths, computations using the grid-sequence capacity of the EllipSys code were performed, producing converged results on five grid resolutions with the coarsest being 64×24 cells. The grid is constructed such that the grid expansion is kept low in the areas of strong gradients, aiming at keeping the cell aspect ratio constant. The computed lift and drag values are reported in Table 1, 3, and 5. Based on these the actual order of the code using Richardson Extrapolation was determined as 2 for laminar flow, 1.6 for fully turbulent flow and 1.8 for transition flow,

see Tables 2, 4 and 6. Due to the highly non-linear behavior of the transition process, a chord wise refined grid of 2048x384 cells was generated where the cell clustering was optimized to capture the transition points, in order to establish the grid convergence order of the transitional computation. For this mesh the off-wall spacing was relaxed to 1×10^{-6} chord lengths. All results used for the grid convergence study are based on solutions where the residuals were reduced more than 7 orders of magnitude, in order to have consistent results for the small changes in the computed values.

Table 1. Grid Refinement study for the NACA64-418 airfoil for the 1024×384 grid, using laminar computations at $Re = 1000$ at 0 deg. angle of attack.

Coarsening Level	C_l	C_d	C_m
16	-0.0027105	0.147217	0.00071599
8	-0.0038302	0.144852	-0.00175911
4	0.0082011	0.144127	0.000554215
2	0.0105299	0.144018	0.00097765
1	0.0111450	0.14399	0.00108387
Richardson	0.0113098	0.143983	0.00111042

Table 2. Estimated order of the algorithm for laminar flow at $Re = 1000$ at 0 deg. angle of attack on the 1048×384 grid, using Richardson Extrapolation.

k	p_{C_l}	p_{C_d}	p_{C_m}
2+4+8	2.4	2.7	2.4
1+2+4	1.9	2.0	2.0

Table 3. Grid Refinement study for the NACA64-418 airfoil for the 1024×384 grid, using fully turbulent computations at $Re = 3 \times 10^6$ and 0 deg. angle of attack.

Coarsening Level	C_l	C_d	C_m
16	0.342502	0.0142428	0.0817013
8	0.343764	0.0109858	0.0817091
4	0.335088	0.0105618	0.0796326
2	0.331054	0.010481	0.0786814
1	0.329704	0.0104599	0.0783661
Richardson	0.329367	0.0104546	0.0782873

Table 4. Estimated order of the algorithm for fully turbulent flow on the 1048×384 grid for fully turbulent flow at 0 deg, using Richardson Extrapolation.

k	p_{C_l}	p_{C_d}	p_{C_m}
2+4+8	1.10	2.39	1.12
1+2+4	1.58	1.94	1.59

The observed variation of the order of the scheme can be explained using the mixed-order analysis. Using the three finest grid levels, the exact solution and the coefficients g_1 and g_2 are estimated. Comparing the behavior of the error between the computed lift value and the extrapolated value using the mixed-order approximation, we see that for the coarsest levels where the magnitude of the third and second order terms are of equal magnitude but opposite

Table 5. Grid Refinement study for the NACA64-418 airfoil for the 2048×384 grid, using transitional computations at $Re = 6 \times 10^6$ and 6 deg. angle of attack.

k	C_l	C_d	C_m
8	1.04093	0.01098340	0.174302
4	1.05689	0.00845596	0.17711
2	1.05317	0.00818944	0.176174
1	1.05216	0.00811763	0.175933
Richardson	1.05178	0.00845598	0.175849

Table 6. Estimated order of the algorithm for the transitional flow on the 2048×384 grid for fully turbulent flow at 6 deg., using Richardson Extrapolation.

Coarsening Level	p_{C_l}	p_{C_d}	p_{C_m}
1+2+4	1.88	1.89	1.95

sign, the order of the scheme behave in non-consistent way see Figure 1 and 2. As should be expected, the second order terms start to dominate over the third order term on the finer meshes, and the accuracy of the scheme clearly approaches the second order behavior from below as the importance of the third order term vanishes.
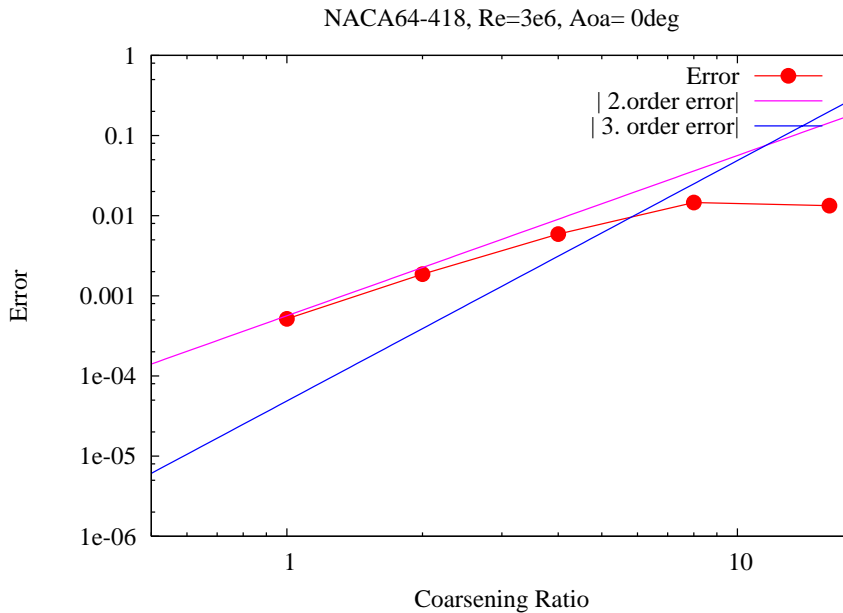

Figure 1. The error in the computed lift for the fully turbulent computation. From the figure it can be seen that for the two coarsest grid levels the second and third order terms are of equal magnitude.

From theoretical considerations, the code should be 2. order accurate based on the discretization of the convective and diffusive terms. But as shown from the mixed-order analysis, the third order terms are still influencing the results at the intermediate grid levels. As shown in Figure 1, the error approaches a second order behavior on the finest meshes. As the order estimation is based on three grid levels, and the solution is still influenced by the third order error, the order estimated by the standard formula is slightly lower than given by the more correct mixed-order approach. Based on the actual established order of the scheme p~ 2, the grid converged solution can be computed by Richardson extrapolation, see Eqn. 6:
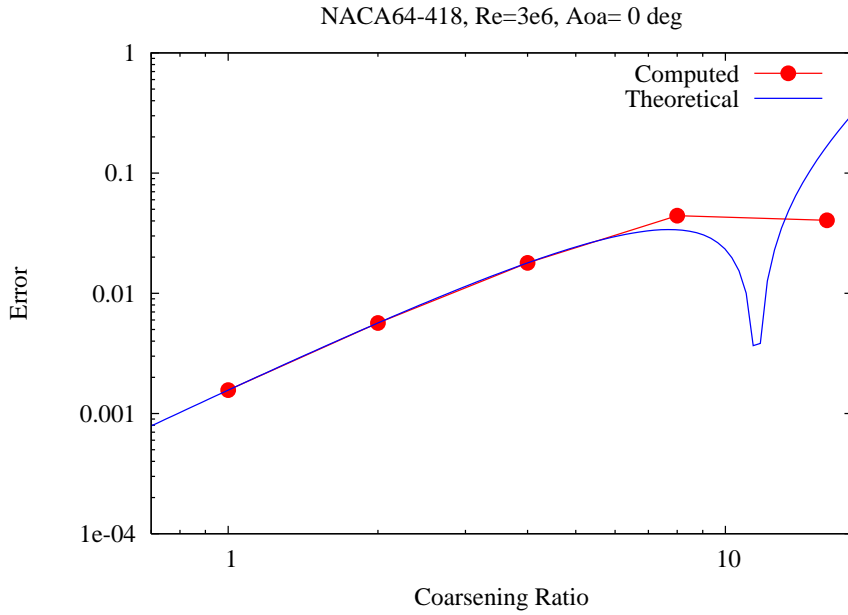
NACA64-418, Re=3e6, Aoa= 0 deg

Figure 2. Comparison of theoretical error variation based on 2 and the variation of the computed error. From the figure it can be seen that for a mesh of 256x96 the error is approximately 3% of the extrapolated value based on Richardson extrapolation.

$$U_{Ext.} = \frac{r^p U1 - U2}{(r^p - 1)} \; , r = 2 \; , \tag{6}$$

where $U1$ is the solution on the finer level and $U2$ is the coarse grid solution. Based on this 'grid converged' solution we can estimate the error on all grid levels. Using this procedure we can estimate the error for the transitional computation using the 256×48 grid to be around 1%, 3% and 1% for the lift, drag and moment respectively, see also Figure 2. We must expect that the error will increase when approaching the more non-linear cases at high angle of attack, but here the chosen 2D assumption of the flow will additionally pose serious problems. Based on these considerations, it was decided to use a grid of 384×384 cells, where the solution behavior should be close to second order.

4 Computational grid

The computational grids around the airfoils are constructed using the HypGrid2D code [17], using 384×384 cells, see Figure 3. The outer boundary is placed approximately 20 chordlengths from the airfoil surface, and the off-wall spacing of the first cell is 1×10^{-6} chord lengths. The stretching in the normal direction is very weak close to the wall, placing the first 256 cells within $\frac{1}{10}$ of the airfoil chord. The outlet is specified on the part of the downstream boundary covering from 40 to 110 degrees, zero being straight above the airfoil.

The meshes used for the grid convergence study are very similar, just with much higher cell count and a weaker stretching. Here, the off wall spacing of the first cell is 1×10^{-7} chord lengths for the laminar and turbulent computations and 1×10^{-6} chord lengths for the transitional ones, and the outlet part of the domain covers the approximate same downstream region.
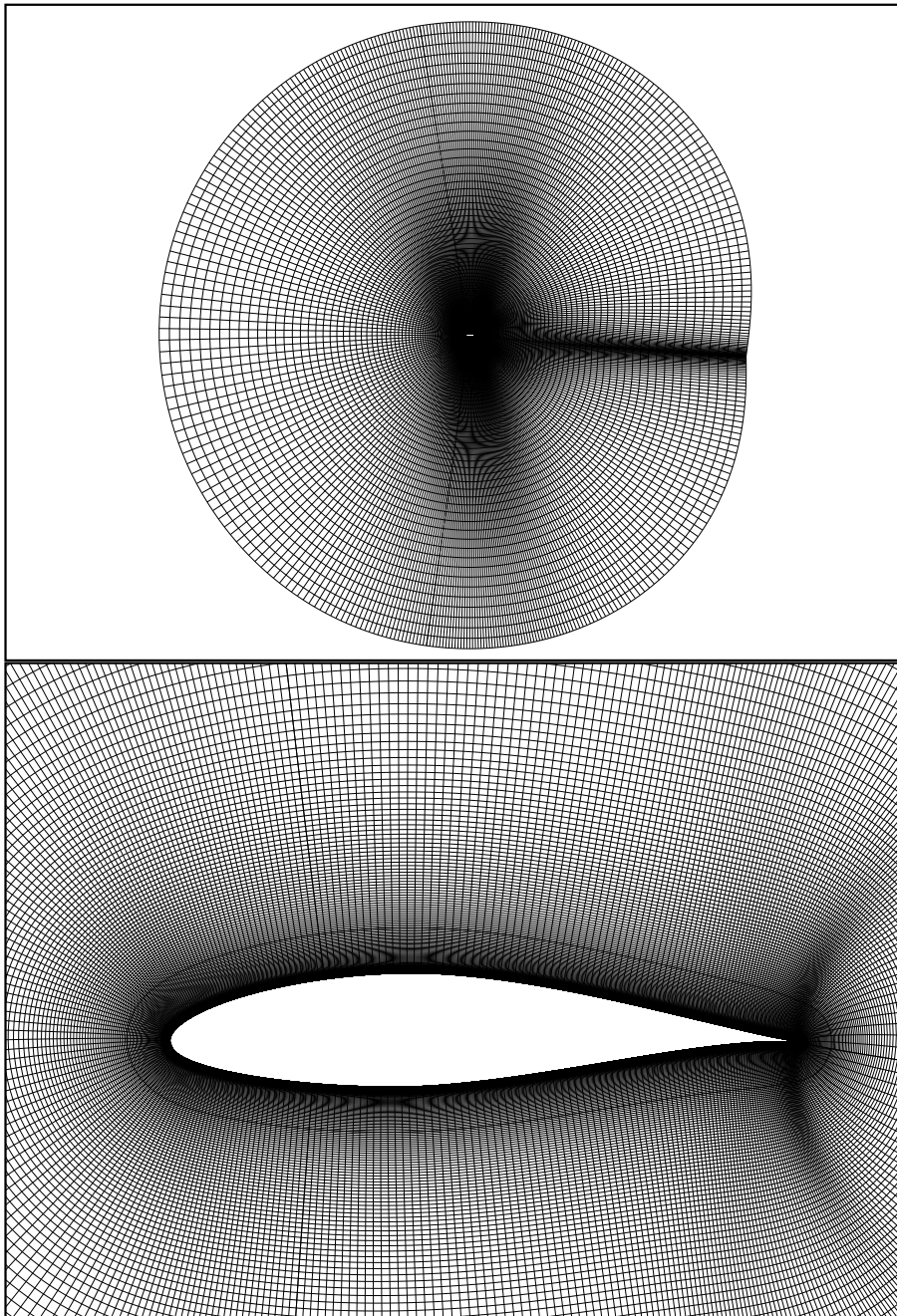
Figure 3. The O-mesh configuration used for the airfoil computations, here shown for the NACA64-418 geometry. The mesh has 384 cells in the chordwise direction and 384 cells in the normal direction.

5 Results

Four airfoils are studied, namely the NACA64-018, 218, 418 and 618. The results computed with the EllipSys2D code are compared with the measurements of Abbott and Doenhoff [4] and computations carried out using the Xfoil code [5]. All computations are performed at a Reynolds number of six million. In the EllipSys2D computations a very low inflow turbulence intensity of 0.01% is used to assure natural transition, similar to what was measured in the NASA LTPT [18].

All computations presented in the present work are performed using steady state computations with under relaxation factors of 0.8, 0.2, 0.7 and 0.7 for momentum, pressure, turbulence and transition equations, respectively, using the SIMPLE algorithm. The convective terms are discritized using the QUICK scheme for the momentum equations and a blend of 60% QUICK and 40% UDS for the turbulent and transitional equations. The computations are performed using a five level grid sequence.

Looking at the computed lift, Figure 4, a very good agreement is observed between measurements and the two computational codes for low angles of attack between -6 and 6 degrees for all airfoils, with the exception of the NACA64-618 airfoil. As also reported by Timmer [19], there seems to be an angle offset in the measurements for this case supported by the present study by the good agreement between the EllipSys and Xfoil results. Looking at the lift/drag curves, similar good agreement is observed, especially at the low lift values. For the lift/drag curves the good agreement with the measured values, are supporting the assumption that the offset observed for the lift as function of angle of attack for the NACA64-618 are caused by an angle offset in the measurements, see Figure 5.

Looking at the deep stall part of the curves, it can be observed that The EllipSys code generally predicts C_l max at slightly lower angles compared to the predictions of Xfoil, but that both computer codes predict higher C_l max than the observed values in the experiment. The experiment was performed for a relatively narrow airfoil section with a ratio of span divided by the chord of only 1.5. The present author has not been able to verify that any boundary layer control (suction/blowing) is applied at the side faces of the LTPT to minimize eventual effects of the developing boundary layers at the side walls in connection with the fairing of the airfoil section with the tunnel walls. The developing boundary layer at the side walls may, especially at high angles of attack, play an important role in the exact development of the stall of the airfoil, introducing highly three-dimensional flow patterns near the fairings with the walls. Another direct indication that the stalling characteristics are not necessarily very accurate can be deduced by comparing the lift at positive and negative angles of attack for a symmetric airfoil, as reported by Timmer [19]. When comparing the negative and positive lift values for the NACA64-018 symmetric airfoil, Timmer demonstrates that the max lift varies around 7%, and attributes this to inaccuracies in the airfoil geometry and angle of attack setting mechanism. For the asymmetrical airfoils, no such simple test can be performed, but similar deviations may be expected.

Comparing the pressure coefficients C_p computed with EllipSys and the Xfoil code, excellent agreement is observed between -6 and 6 degrees, for all four airfoils, see Figure 6 to 9. Looking at the skin friction, the general trend is that the EllipSys code predicts transition slightly aft of the prediction by the Xfoil code in regions of accelerating flow as observed in the leading edge region on the suction side. The EllipSys code predicts the transition location slightly upstream of the location predicted by the Xfoil code in the decelerating regions at the aft part of the suctions and pressure side the airfoil. This could suggest that the empirical expressions for determining the transition location is to sensitive to the acceleration parameters or pressure gradients, at least compared to the Xfoil model.

The performance of the Xfoil code is well known, and along with previous work the present work indicates that the EllipSys CFD code produces the same level of accuracy. Combining this with the additional possibilities of an general purpose CFD solver: The fact that these codes can be used both for 2D and full 3D computations. The codes can be used in both steady and unsteady mode. The fact that any type of geometry can be investigated, from cylinders, flat-back airfoils, to geometries with dynamic actuators such as micro-taps and flaps. All this provides us with a very general tool, for investigating different aerodynamic aspects of relevance for wind turbine applications, with an accuracy comparable to the accuracy of the 2D steady Xfoil code.
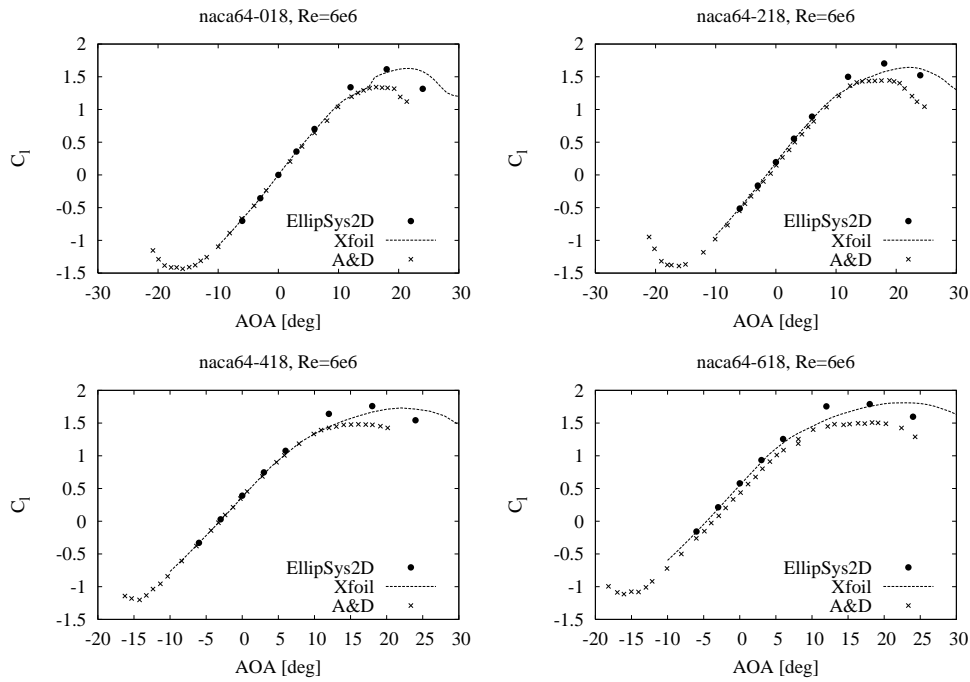
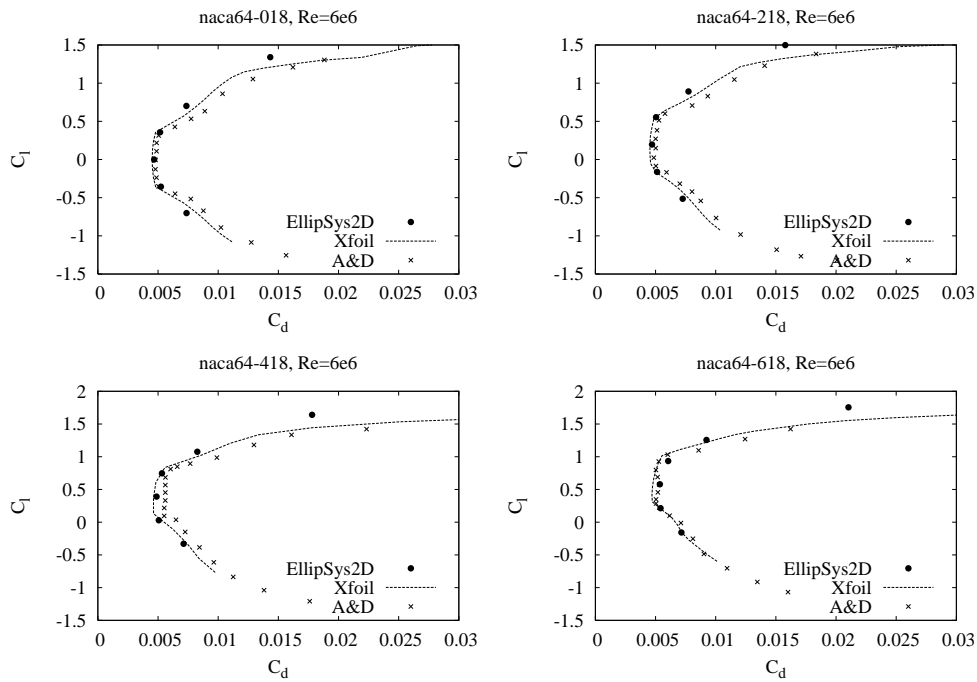*Figure 4. Computed lift for the four NACA64-x18 airfoils.*

Figure 5. Computed lift/drag for the four NACA64-x18 airfoils.

6   Conclusion

The accuracy and grid convergence of the implemented $\gamma - Re_\theta$ correlation based transition model in the EllipSys code is investigated, and the model is applied to four airfoils of the NACA-64-XXX family, the 018, 218, 418 and 618. Using the mixed order error analysis, the
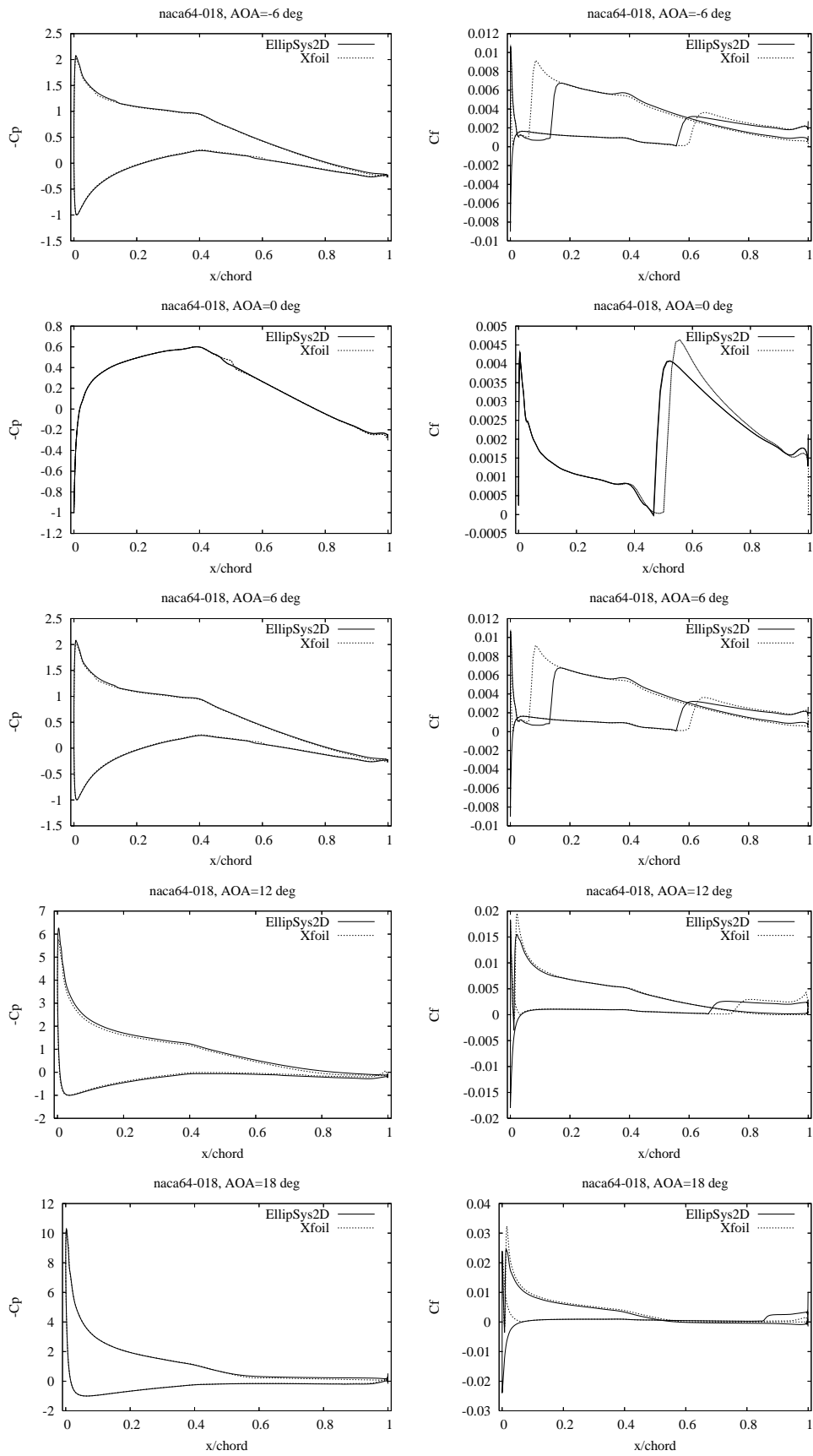
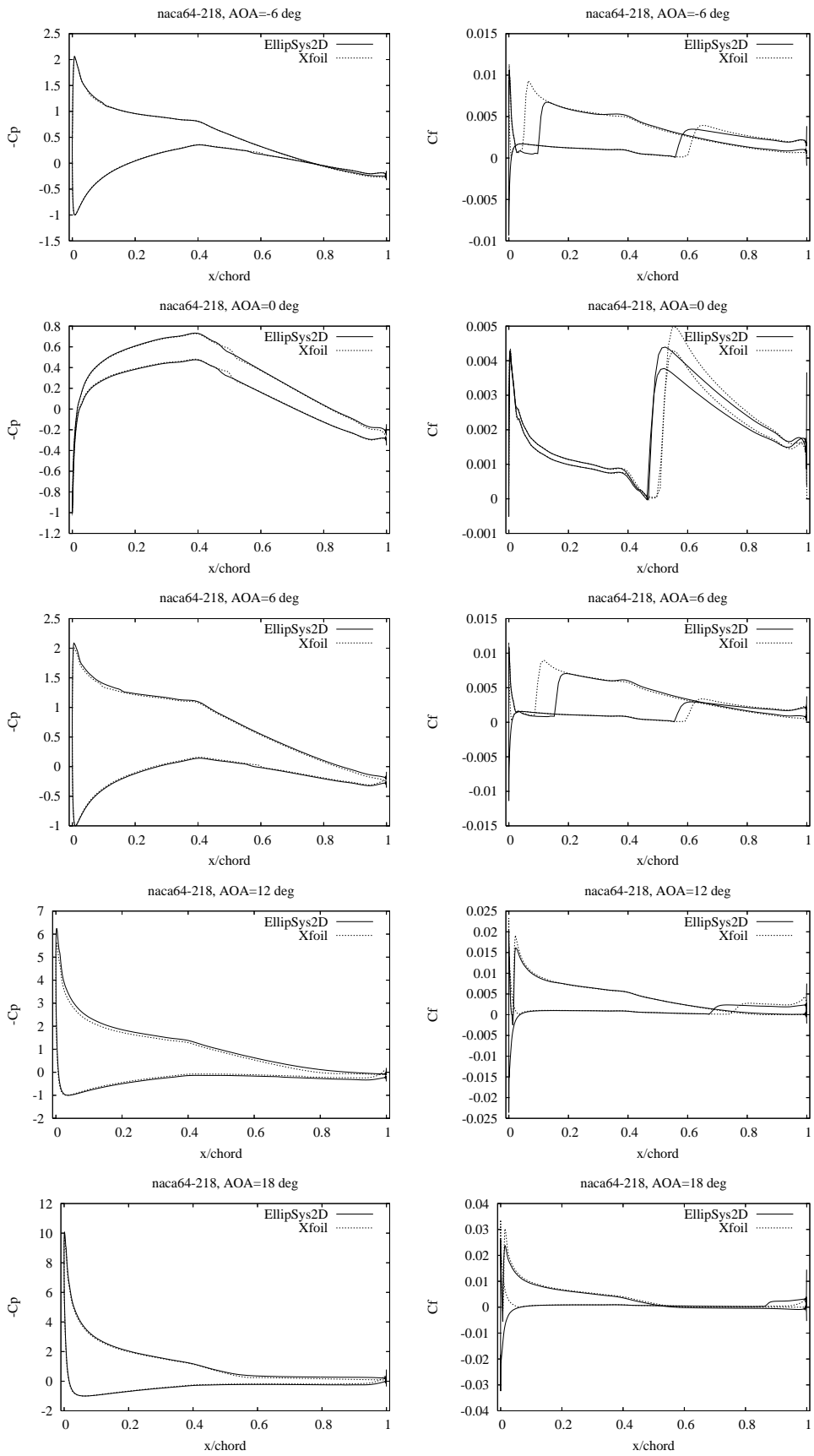*Figure 6. C_p and C_f distributions for the NACA64-018 airfoil.*

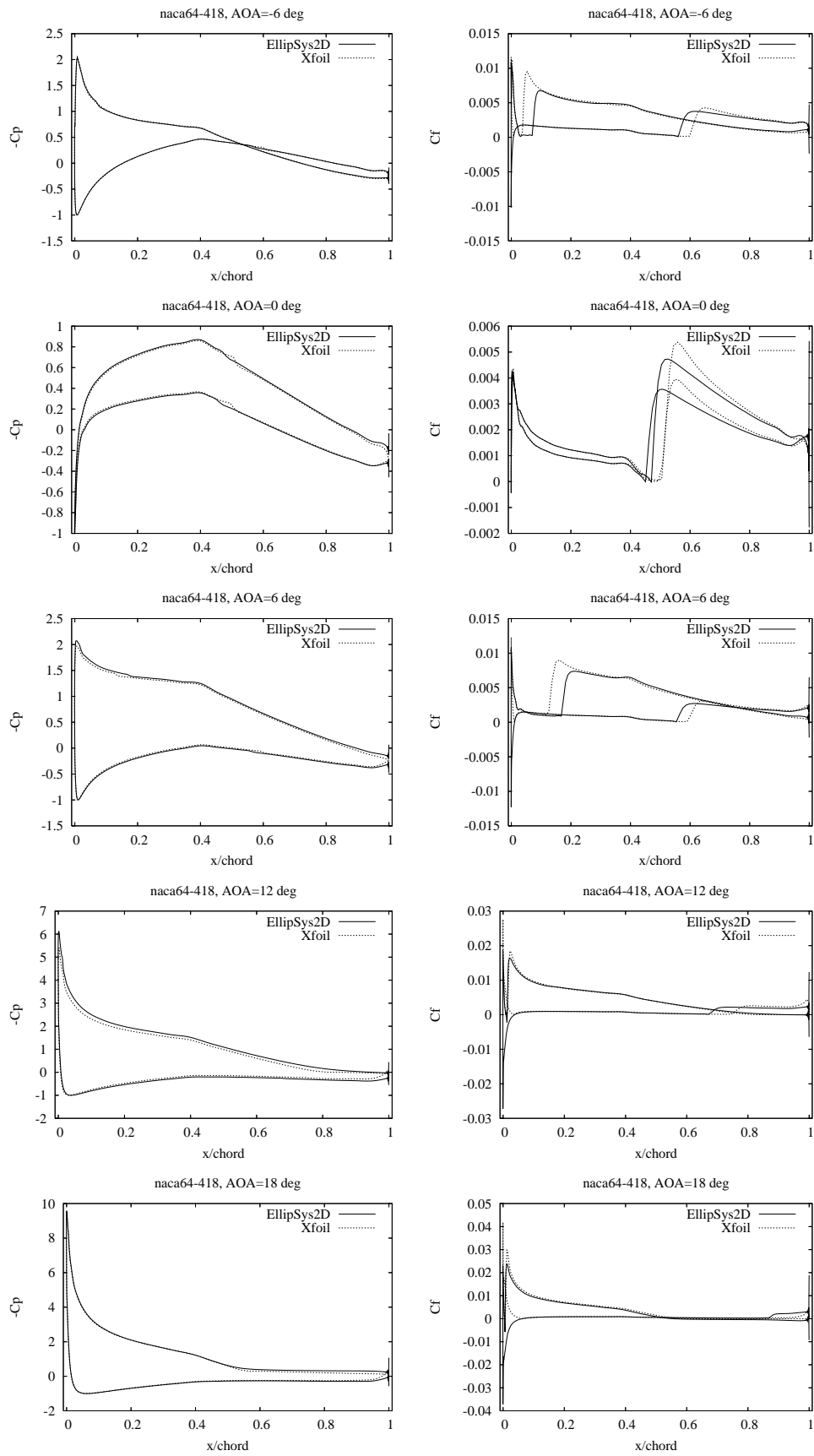*Figure 7. C_p and C_f distributions for the NACA64-218 airfoil.*

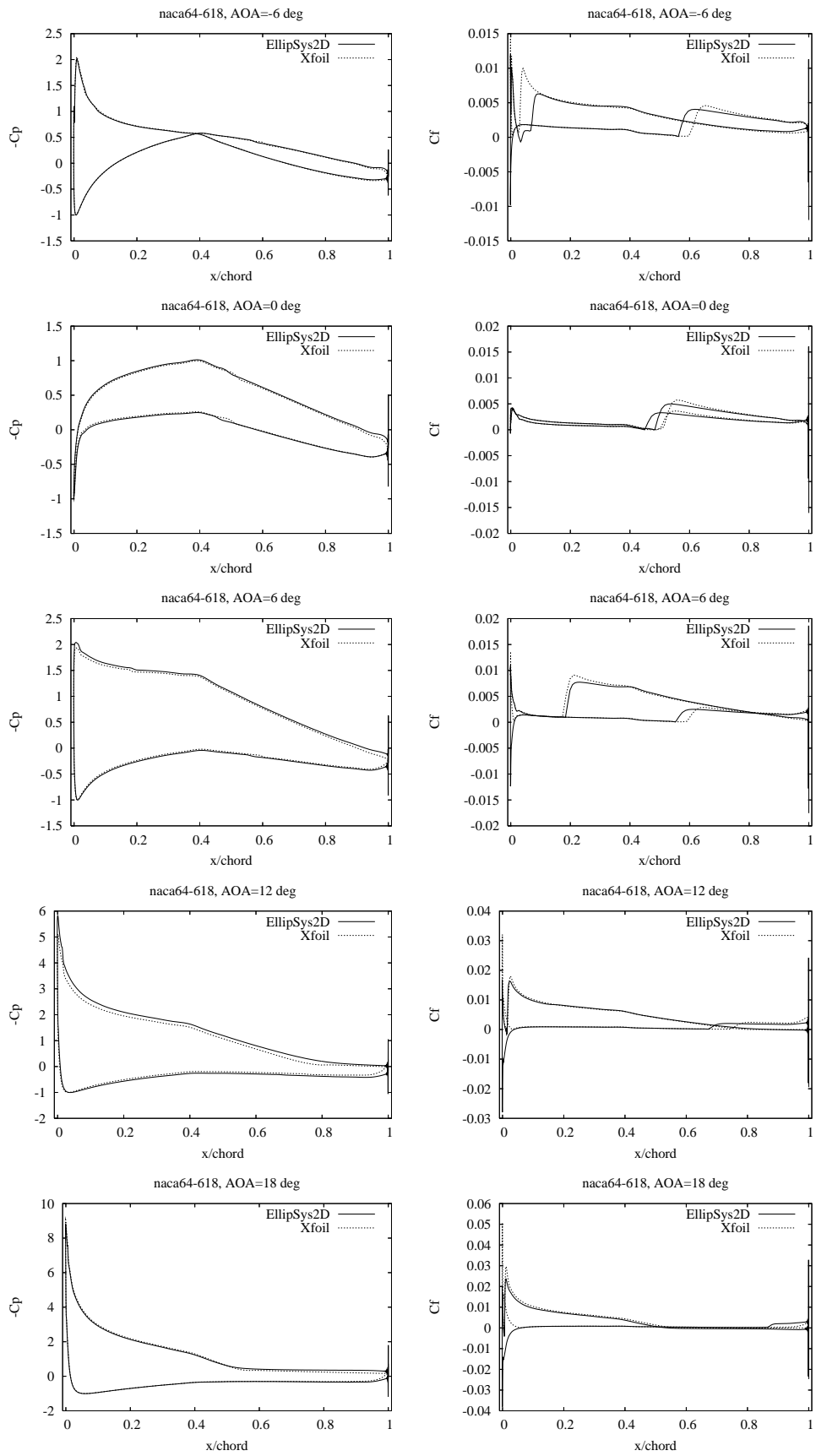*Figure 8. C_p and C_f distributions for the NACA64-418 airfoil.*

Figure 9. C_p and C_f distributions for the NACA64-618 airfoil.

expected second order accuracy of the code is verified, clearly supporting that both the laminar, turbulent and transitional models are correctly implemented from a numerically point of view. Next, looking at the computed lift and drag a very good agreement is observed between measurements, Xfoil computations and predictions by the Ellipsys code for low angles of attack between -6 and 6 degrees for all airfoils, with the exception of the NACA64-618 airfoil. As also reported by Timmer, there seems to be an angle offset in the measurements for this case supported by the present study by the good agreement between the EllipSys and Xfoil results. Looking at the lift/drag curves similarly good agreement is observed, especially at the low lift values. For the lift/drag curves the good agreement with the measured values support the assumption that the offset observed for the lift as function of angle of attack for the NACA64-618 is caused by an angle offset in the measurements. The performance of the Xfoil code is well known, and along with previous work the present work indicates that the EllipSys CFD code produces the same level of accuracy. With the additional possibilities of a general purpose 3D steady/unsteady CFD solver, a versatile tool for investigating different aspects of wind turbine aerodynamics is available.

7   Acknowledgement

References

[1] F. R. Menter, R. B. Langtry, S. R. Likki, Y. B. Suzen, P. G. Huang, and S. Völker. A Correlation-Based Transition Model Using Local Variables, Part I - Model Formulation. In *Proceedings of ASME Turbo Expo 2004, Power for Land, Sea, and Air*, Vienna, Austria, June 14-17 2004. ASME. GT2004-53452.

[2] F. R. Menter, R. B. Langtry, S. R. Likki, Y. B. Suzen, P. G. Huang, and S. Völker. A correlation-based transition model using local variables, part ii - test cases and industrial applications. In *Proceedings of ASME Turbo Expo 2004, Power for Land, Sea, and Air*, Vienna, Austria, June 14-17 2004. ASME. GT2004-53454.

[3] N. N. Sørensen. CFD modeling of laminar-turbulent transition for airfoils and rotors using the gamma - Retheta model. In *2008 European Wind Energy Conference and Exhibition*, , pages 106–112, Brussels (BE), 31 Mar - 3 Apr 2008 2008. EWEC.

[4] I. H. Abbott and A. E. von Doenhoff. *Theory of Wing Sections*. Dover Publications, Inc., New York, 1959.

[5] M. Drela and M. B. Giles . Viscous-Inviscid Analysis of Transonic and Low Reynolds Number Airfoils. *AIAA Journal*, 25(10):1347–1355, October 1987.

[6] J. A. Michelsen. Basis3D - a Platform for Development of Multiblock PDE Solvers. Technical Report AFM 92-05, Technical University of Denmark, 1992.

[7] J. A. Michelsen. Block structured Multigrid solution of 2D and 3D elliptic PDE's. Technical Report AFM 94-06, Technical University of Denmark, 1994.

[8] N. N. Sørensen. General Purpose Flow Solver Applied to Flow over Hills. Risø-R- 827-(EN), Risø National Laboratory, Roskilde, Denmark, June 1995.

[9] C. M. Rhie. *A numerical study of the flow past an isolated airfoil with separation*. PhD thesis, Univ. of Illinois, Urbana-Champaign, 1981.

[10] S. V. Patankar and D. B. Spalding. A Calculation Prodedure for Heat, Mass and Momentum Transfer in Three-Dimensional Parabolic Flows. *Int. J. Heat Mass Transfer*, 15:1787, 1972.

[11] S. V. Patankar. *Numerical Heat Transfer and Fluid Flow*. Hemisphere Publishing Corporation, 1980. ISBN: 0891165223.

[12] R. I. Issa. Solution of the Implicitly Discretised Fluid Flow Equations by Operator-Splitting. *J. Computational Phys.*, 62:40–65, 1985.

[13] R. I. Issa, A. D. Gosman, and A. P. Watkins. The Computation of Compressible and Incompressible Recirculating Flows by a Non-iterative Implicit Scheme. *J. Computational Phys.*, 62:66–82, 1986.

[14] P. K. Khosla and S. G. Rubin. A diagonally dominant second-order accurate implicit scheme. *Computers Fluids*, 2:207–209, 1974.

[15] F. R. Menter. Zonal Two Equation k-ω Turbulence Models for Aerodynamic Flows. AIAA-paper-932906, 1993.

[16] C.J. Roy. Grid Convergence Error Analysis for Mixed-Order Numerical Schemes. *AIAA JOURNAL*, 41(4):595–604, April 2003.

[17] N. N. Sørensen. HypGrid2D a 2-D Mesh Generator. Risø-R- 1035-(EN), Risø National Laboratory, Roskilde, Denmark, Feb 1998.

[18] A.E. von Doenhoff and Jr. F.T. Abott. Technical report.

[19] W.A. Timmer. An overview of NACA 6-digit airfoil series characteristics with reference to airfoils for lage wind turbine blades. AIAA Paper 2009-268, 2009.

Risø DTU is the National Laboratory for Sustainable Energy. Our research focuses on development of energy technologies and systems with minimal effect on climate, and contributes to innovation, education and policy. Risø has large experimental facilities and interdisciplinary research environments, and includes the national centre for nuclear technologies.